Journal Pre-proofs

3D Printed Bilayer Tablet with Dual Controlled Drug Release for Tuberculosis Treatment

Atabak Ghanizadeh Tabriz, Uttom Nandi, Andrew P. Hurt, Ho-Wah Hui, Shyam Karki, Yuchuan Gong, Sumit Kumar, Dennis Douroumis

PII: S0378-5173(20)31132-7
DOI: https://doi.org/10.1016/j.ijpharm.2020.120147
Reference: IJP 120147

To appear in: *International Journal of Pharmaceutics*

Received Date: 14 November 2020
Revised Date: 28 November 2020
Accepted Date: 30 November 2020

Please cite this article as: A. Ghanizadeh Tabriz, U. Nandi, A.P. Hurt, H-W. Hui, S. Karki, Y. Gong, S. Kumar, D. Douroumis, 3D Printed Bilayer Tablet with Dual Controlled Drug Release for Tuberculosis Treatment, *International Journal of Pharmaceutics* (2020), doi: https://doi.org/10.1016/j.ijpharm.2020.120147

This is a PDF file of an article that has undergone enhancements after acceptance, such as the addition of a cover page and metadata, and formatting for readability, but it is not yet the definitive version of record. This version will undergo additional copyediting, typesetting and review before it is published in its final form, but we are providing this version to give early visibility of the article. Please note that, during the production process, errors may be discovered which could affect the content, and all legal disclaimers that apply to the journal pertain.

© 2020 Published by Elsevier B.V.

3D Printed Bilayer Tablet with Dual Controlled Drug Release for Tuberculosis Treatment

Atabak Ghanizadeh Tabriz[1,2], Uttom Nandi[1,2], Andrew P. Hurt[1], Ho-Wah Hui[3], Shyam Karki[3], Yuchuan Gong[3*], Sumit Kumar[3*], Dennis Douroumis[1,2*]

[1]Faculty of Engineering and Science, School of Science, University of Greenwich, Chatham Maritime, Chatham, Kent ME4 4TB, UK

[2]CIPER Centre for Innovation and Process Engineering Research, Kent, ME4 4TB, UK

[3] Drug Product Development, Bristol Myers Squibb (formerly Celgene Corporation), 556 Morris Avenue, Summit, NJ 07901, USA

Journal Pre-proofs

*Corresponding Authors

Dennis Douroumis, Professor in Pharmaceutical Technology and Process Engineering, Chatham Maritime, Chatham, Kent ME4 4TB, UK, D.Douroumis@gre.ac.uk,

Sumit Kumar, Principal Scientist, Bristol Myers Squibb (formerly Celgene Corporation), Sumit.Kumar@bms.com

Yuchuan Gong, Director, Bristol Myers Squibb (formerly Celgene Corporation), Yuchuan.Gong@bms.com

Abstract

In this study Fusion Deposition Modelling (FDM) was employed to design and fabricate a bilayer tablet consisting of isoniazid (INZ) and rifampicin (RFC) for the treatment of tuberculosis. INZ was formulated in hydroxypropyl cellulose (HPC) matrix to allow drug release in the stomach (acidic conditions) and RFC was formulated in hypromellose acetate succinate (HPMC – AS) matrix to allow drug release in the upper intestine (alkaline conditions). This design may offer a better clinical efficacy by minimizing the degradation of RFC in the acidic condition and potentially avoid drug-drug interaction. The bilayer tablet was prepared by fabricating drug containing filaments using hot melt extrusion (HME) coupled with the 3D printing. The HME and 3D printing processes were optimized to avoid drug degradation and assure consistent deposition of drug-containing layers in the tablet. The in-vitro drug release rate was optimized by varying drug loading, infilling density, and covering layers. Greater than 80% of INZ was released in 45 mins at pH 1.2 and approximately 76% of RFC was releases in 45 mins after the dissolution medium was changed to pH 7.4. The work illustrated the potential application of FDM technology in the development of oral fixed dose combination for personalized clinical treatment.

Keywords: 3D printing, oral solid dosage forms, controlled release, isoniazid, rifampicin, tuberculosis.

Journal Pre-proofs

1. Introduction

3-Dimensional (3D) printing as an emerging technology has drawn a significant attention in the field of medicine particularly in drug delivery. Various 3D printing technologies, such as Fused Deposition Modelling (FDM) (Gioumouxouzis et al., 2020; Goyanes et al., 2015a; Melocchi et al., 2019; Scoutaris et al., 2018; Siamidi et al., 2020; Zema et al., 2017), selective laser sintering (Fina et al., 2018, 2017), and inkjet printing (Kyobula et al., 2017), have been successfully employed and shown great potential in personalised medicines ((Trenfield et al., 2018)).

Fused deposition modelling 3D printing has been the frontier additive manufacturing technology (Aho et al., 2019; Nasereddin et al., 2018)applied to personalised oral dosage forms. Besides its low cost, the technology can be used with majority of the pharmaceutically accepted polymers, such as methacrylate (Sadia et al., 2016), various cellulose (Michael et al., 2013) – (Chai et al., 2017), and poly lactic acid (Boetker et al., 2016)

Aita *et al*. employed pressure-assisted micro-syringe printing method (PAM) to fabricate levetiracetam immediate release tablets. All printed tablets presented fast disintegration within 95 – 120 seconds. The tablets comprised of semi-solid polyvinyl alcohol (PVA) and polyethylene glycol exhibited a complete drug release within only 10 min, while those comprised of polyvinylpyrrolidone-vinyl acetate copolymer (PVP-VA) showed a slightly slower drug release (El Aita et al., 2019).

Linares *et al.* developed a 3D printing platform by combining FDM and injection volume filling to prepare customized extruded scaffolds followed by the injection of liquid or semi-solid systems. The versatile printing technology was used to fabricate tablets with various drug release profiles (Pietrzak et al., 2015). Several studies demonstrated that 3D printed tablets with lower infill density have faster drug release due to their higher surface area (Goyanes et al., 2015a; Jamróz et al., 2018; Sadia et al., 2018). These works suggested that 3D printing can be used to prepare personalised medicine by manipulating the infill density of a tablet.

Incorporation of multiple drugs in a single dosage form may improve patient's compliance and minimize administration errors (Bangalore et al., 2007; Castellano et al., 2014; Pereira et al., 2019). Pereira *et al.* demonstrated the application of the 3D printing technology in the medicines consist of multiple drugs (Pereira et al., 2019). The authors printed a polypill consisting of three active pharmaceutical ingredients (API's), i.e. indapamide, rosuvastatin

calcium, and amlodipine besylate using FDM technology, and optimized the release profile of each API by simply adjusting the placement of the API within the polypill.

Only few studies have reported the use of FDM as a tool to generate personalised bilayer tablets with controlled drug release profiles (Gioumouxouzis et al., 2018; Goyanes et al., 2015b). Gioumouxouzis *et al*. prepared bilayer tablets consisting metformin and glimepiride using FDM technology for treatment of type II diabetes. The researchers used different polymers in each layer to generate an immediate release profile for glimepiride and a prolonged release profile for metformin (Gioumouxouzis et al., 2018). In another study, similar approach was used to prepare a bilayer tablet consisting paracetamol with immediate release profile and caffeine with a delayed release profile (Goyanes et al., 2015b).

According to the World Health Organization (WHO), tuberculosis (TB) is one of the lethal infectious diseases affected approximately 10 million people with approximately 1.2 million fatality in 2018. Rifampicin (RFC) and isoniazid (INZ) are two antibiotics used as first line treatment for TB. H. Öblom *et al.* prepared INZ tablets using FDM technology (Öblom et al., 2019). The authors manipulated the release of INZ from the tablets by varying the type of polymer in the formulation.

Oral fixed dose combination (FDC) tablets of RFC and INZ would significantly enhance patient compliance, especially in the areas TB is widely spread (Horsburgh et al., 2015), (Blomberg et al., 2001). The two drugs need to be released from a FDC tablet with a lag time to avoid the drug-drug interaction which causes the degradation of the drugs (Shishoo et al., 2001a). Genina *et al.* designed a 3D printed tablet with two compartments using polylactic acid (PLA) as the matrix (Genina et al., 2017). RFC and INZ drug substances were manually fed into separate compartments. The compartment consisting RFC was exposed to dissolution medium, thus, exhibited a fast drug release, i.e. 80 – 90% of RFC released in 1 hour. The compartment consisting INZ was sealed with a polyvinyl alcohol (PVA) cap, which delayed the release of INZ by 2 hours in acidic media and exhibited a sustained release in alkaline media. Such a design allows a delay between the release of the two drugs when administered. A drawback of this novel approach is that PLA is not a compendial excipient. In addition, rifampicin and isoniazid drug substance were manually fed into each compartment, which may create significant variability during manufacturing.

It is desired to develop a novel RFC/INZ FDC tablet with distinguished drug release profiles that reduce undesirable drug interactions after administration and can be consistently be

manufactured. In this study, we designed 3D printed bilayer tablets with isoniazid and rifampicin released at different pH to avoid drug-drug interactions. RFC/hydroxypropyl methylcellulose acetate succinate and INZ/hydroxypropyl cellulose filaments were prepared by hot melt extrusion (Aho et al., 2019). The filaments were then used to fabricate the FDC tablet by FDM 3D printing.

2. Materials and Methods

2.1 Materials

Isoniazid (INZ) and polyethylene glycol 6000 (PEG) were purchased from Sigma-Aldrich (UK). Rifampicin (INH) was purchased from Tokyo Chemical (Belgium). Hydroxypropyl methylcellulose acetate succinate (HPMCAS, AQOAT® AS-LMP) and hydroxypropyl cellulose (HPC, Klucel® EF) were kindly donated by Shin–Etsu (Japan) and Ashland (Netherlands), respectively.

2.2 Hot melt extrusion for filaments

Three filaments were prepared using hot melt extrusion. The compositions of the three filaments utilized in this study were RFC/HPMCAS/PEG (35/45/20, w/w%), RFC/HPMCAS/PEG (25/55/20, w/w%) and INZ/HPC (25/75, w/w%). PEG was added to the RFC/HPMCAS filament, as a plasticizer to enable extrusion at lower temperature and thus minimize degradation of RFC.

Physical mixtures of the drug substance and the corresponding polymer/plasticiser were blended in a Turbula shaker-mixer (Glen Mills T2F Shaker/Mixer, USA) at 75 rpm for 10 minutes to create common blends. The blends were fed into a 16 mm twin-screw extruder (Eurolab 16, Thermo Fisher, Germany) at a controlled feed rate of 10 g/min. The extruded melt flows through a circular die with 3 mm diameter to form the filament. The screw speed was set at 50 rpm while the conveying speed was adjusted to achieve filaments with a desired thickness of 2.6 - 2.9 mm. Extrusion settings with drug/polymer ratios, temperature profiles, and screw rates are shown in supplementary materials (Tables 1, 2).

2.3 Design and 3D printing of tablets

Tablets were designed with SolidWorks software V20 (Dassault Systems, USA). The designs were converted into stereolithography .stl files and sliced by Cura software version 4.0 (Ultimaker, Netherland) which generates the printing path for the 3D printer. Tablets were printed using an Ultimaker 3 extended (Ultimaker, Netherland), a dual extruder FDM printer

equipped with a 0.4 mm print core (0.4 mm printing nozzle). The layer consisting INZ and RFC was printed at optimized temperatures of 130 °C and 170 °C, respectively (data not shown). The printing was carried out with a layer height of ~ 0.1 mm at a speed of 20 mm/s.

All 3D-printed tablets consist 100 mg of RFC in one layer and 100 mg of INZ in another. Active formulations were printed into tablets with empty spaces to create various tablet infill density, thus modify the drug release. To further reduce the drug release in some tablets, the most exterior layers of the active tablets were printed without empty space as covering layers. The length and width of the tablets were fixed at 22 mm and 9.5 mm, respectively. The height of INZ tablets ranged from 3.5-5.2 mm and RFC tablets varied between 3-4.5 mm depending on the infill density and presence of covering layers (Table 1).

Table 1. Tablet design for Isoniazid and Rifampicin formulations. All designs presented 22 mm length and 9.25 mm width.

Design	API	Polymer/ plasticizer	Height (mm)	Number of Covering layers	Infill Density (%)	Drug loading %
1	INZ	HPC	3.5	3	55	25
2	INZ	HPC	4	1	60	25
3	INZ	HPC	4.5	0	60	25
4	INZ	HPC	5.2	0	45	25
5	RFC	HMPCAS/PEG	3.5	3	55	25
6	RFC	HMPCAS/PEG	4	1	60	25
7	RFC	HMPCAS/PEG	4.5	0	60	25
8	RFC	HMPCAS/PEG	3	0	60	35
9	RFC	HMPCAS/PEG	3.5	0	50	35
10	RFC	HPMCAS/PEG	4.5	0	30	35

2.4 Thermal Gravimetric Analysis (TGA)

Thermal stability of the extruded filaments and each individual component were evaluated using a thermal balance (Q5000, TA instruments, USA) equipped with a data analyser (Universal Analysis 2000, version 4.5A, TA instruments, USA). Temperature of TGA furnace was calibrated using curie points of alumel and nickel. During experiments, the furnace was purged with nitrogen at 50 mL/min and the balance chamber was purged at 50 mL/min. Approximate 2 - 2.5 mg of sample was weighed into an aluminium pan. The sample was heated from 25 °C to 400 °C at a rate of 10 °C/min.

2.5 Differential Scanning Calorimetry (DSC)

Thermal behaviour of the extruded filaments both loaded and unloaded including each individual component were collected using a differential scanning calorimeter (Mettler-Toledo 823e, Switzerland) equipped with STARe Excellence Thermal Analysis Software version 9.0. The temperature axis was calibrated with biphenyl, indium, and tin standards. The cell constant was calibrated with indium. Approximate 2 - 2.5 mg of sample was weighted into a 40 µL sealed aluminium pan and crimp-closed. Samples containing INZ were heated from -30 °C to 230 °C at a heating rate 10°C/min. All other samples were heated from -30 °C to 300 °C at a heating rate of 10 °C/min.

2.6 Scanning Electron Microscopy (SEM)

Scanning electron microscopy (Hitachi SU8030, Japan) was used to evaluate the surface of the filament and the 3D printed bilayer tablets. Samples were secured to aluminium stubs using conductive carbon adhesive tape (Agar Scientific, Stansted, UK) and examined uncoated SEM images were captured by electron beam accelerating voltage of 1KV and 30X to 70X magnification.

2.7 X-Ray powder diffraction (XRPD)

XRPD data were collected using a D8 Advance X-ray Diffractometer (Bruker, Germany) equipped with a LynxEye silicon strip position sensitive detector and parallel beam optics. The diffractometer was operated with a Cu Kα radiation at 40kV and 40mA. The instrument was computer controlled using XRD commander software (Version 2.6.1, Bruker AXS, Germany) and the data was analysed using the EVA software (Version 5.2.0.3, Bruker AXS, Germany). The sample was ground using a mortar and pestle and placed into an aluminium sample holder. Diffraction data was collected between 2 - 60^{o}/2θ with a step size of 0.02^{o} and a counting time of 0.3 seconds per step.

2.8 Energy Dispersive X-ray (EDX)

Energy Dispersive X-ray technique was used to evaluate the drug distribution within the 3D printing filaments. The samples were characterised using a cold-cathode field emission gun SEM (Hitachi SU8030, Japan) and a Thermo-Noran (USA) EDX system with Ultra-Dry 30 mm^2 window. A Noran System 7 software suite containing COMPASS and XPhase was attached. Samples were placed on double-sided adhesive carbon tabs and surface analysis were carried out on SEM images taken at a standard nominal magnification of 250X. The

accelerating voltage for X-ray intensity measurement and SEM observation was 8 kV. Data were extracted using the Compass software.

2.9 *In vitro* dissolution and HPLC analysis

Dissolution of the 3D printed caplets were performed in 900 ml of dissolution medium at 37 ± 1 ^{o}C using a USP II paddle apparatus (Varian 705 DS, USA) with a paddle speed of 100 rpm. Isoniazid tablets were tested in 0.1 N HCl solution (pH 1.2), and rifampicin tablet were tested in 0.4% sodium dodecyl sulphate solution (pH 7.0). All dissolution studies carried out in triplicate. Aliquots of 2 ml samples were withdrawn with replacement at 30, 45, 60, 90, and 120 min. Samples were filtered using 200 μm filter and properly diluted prior to analysis. the concentration of drug in each sample was determined based on the absorption at 254 nm using a high-performance liquid chromatographic system (Agilent Technologies, 1200 series, USA) equipped with a HICHROM S5ODS2-4889 (5×150×4 mm) column and an UV detector. The mobile phase was prepared using methanol/di-sodium hydrogen phosphate (70/30, v/v) and pumped at a flow rate of 1.0 mL/min. Calibration curves were prepared using isoniazid and rifampicin in deionised water and dimethyl sulfoxide respectively at a concentrations of 100, 200, 300, 400, and 500 μg/mL.

3. Results and Discussion

3.1 Tablet design and 3D printing

Previous studies have shown that a combined therapy of INZ and RFC resulted in an improved clinical efficacy in TB treatment (Deardorff and Grossberg, 2016; Gohel and Sarvaiya, 2007). However, a major clinical challenge with such a combined therapy is the poor bioavailability of RFC because it degrades in acidic medium (Genina et al., 2017; Gohel and Sarvaiya, 2007; Shishoo et al., 2001a) and the presence of INZ accelerates the reaction. Genina *et al.* designed a 3D printed tablet that releases RFC in gastric medium and INZ in intestinal medium to improve the bioavailability of RFC. However, this tablet does not prevent the degradation of RFC in acidic medium. We designed a 3D printed bilayer tablet that releases INZ in gastric medium and RFC in upper intestine. This design further reduces the degradation of RFC while still avoids the undesired interaction between the two drugs (Shishoo et al., 2001b). In this bilayer tablet, INZ was formulated with HPC, a non–ionic hydrophilic polymer, to ensure a

fast drug release in acidic medium. RFC was formulated with HPMCAS, an ionic polymer. HPMCAS is a mixture of acetic acid and mono-succinic acid esters of hydroxypropylmethyl cellulose, which is insoluble in acidic medium but swells and dissolves rapidly above pH 5.5. Thus, the release of RFC is expected to be delayed to upper small intestine when formulated in a HPMCAS matrix.

The 3D printed bilayer tablets consisted two active layers, one containing 100 mg INZ and the other containing 100 mg RFC. Empty spaces were created in the tablets during 3D printing to modify infill density. The drug release from the tablets were modified by infill density, covering layer, and/or drug load. The tablets with lower infill density had more empty spaces and higher surface areas, thus higher drug release while exposed to dissolution media. Some formulations were printed without empty spaces (maximum infill density) in their most exterior layers as covering layers. The drug load in the RFC/HPMCAS/PEG formulations was also varied between 25% and 35% to modify the drug release. The individual tablets, with fixed length (22 mm) and width (9.25 mm), had heights varied between 3.0 mm and 5.2 mm depending on the infill density and presence of covering layers. The images of the tablet designs in Table 1 are shown in Fig. 3.

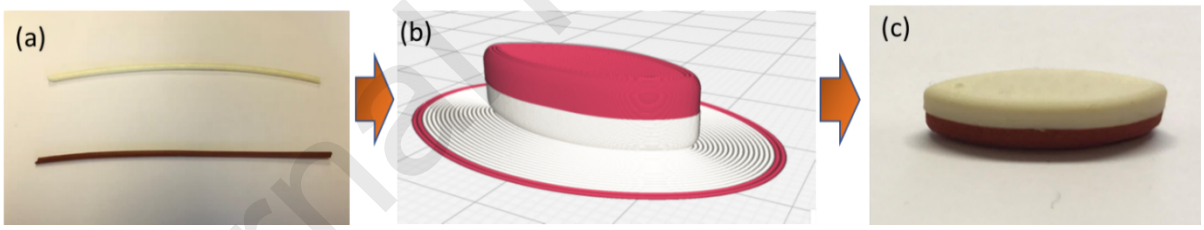

Fig. 1: *Procedure for fabrication of bilayer tablet. (a) Hot melt extruded isoniazid filament (top) and rifampicin 3D printing filaments (bottom). (b) Design and slicing of the bilayer tablet. (c) 3D printed bilayer tablet by FDM.*

The tablets were prepared by hot melt extrusion coupled with FDM 3D printing. The mixtures of INZ/HPC and RFC/HPMCAS/PEG at desired ratios were pre-blended and extruded into filaments (Fig. 1a). The filaments were further printed into a single- or bi-layer tablet by FDM 3D printing (Figure 1c). The print time was approximately 10 – 11 min for the formulations with 25% drug load and 8 – 9 min for those with 35% drug load. The total print time for the optimized bilayer tablet containing both INZ and RFC formulations was approximately 18 minutes.

Genina et al (2017) developed dual - compartment dosage unit for the controlled delivery of the same APIs. Though the approach was novel it comprise of several steps in order to allow physical separation of the loaded APIs. In contrast, our approach is simpler and the designed bilayer tablets can be printed in one go by using simultaneously both extruded filaments.

The thermal stability of the drugs, polymers, and their mixtures were evaluated to determine the maximum temperature below which hot melt extrusion process and 3D printing should be carried out. The TGA data (Fig. 2) showed that INZ and HPC remained thermally stable below ~ 170^{o}C and ~ 200^{o}C, respectively. INZ/HPC (25/75, w/w%) mixture exhibited an onset degradation temperature similar to that of INZ alone. RFC remained thermally stable till it was heated to ~ 240^{o}C.

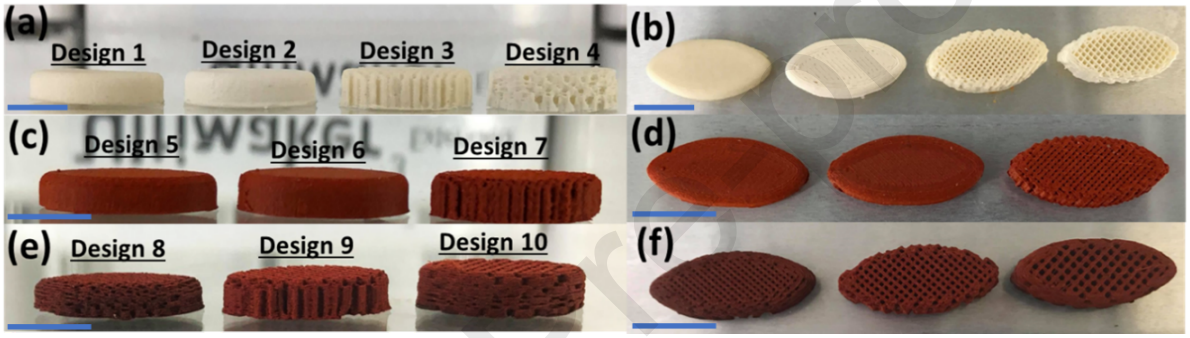

Fig. 2: 3D printed Isoniazid caplet; (a) side view and (b) top view. 3D printed 25% rifampicin loaded caplet: (c) side view and (d) top view. 3D printed 35% rifampicin loaded caplet: (e) side view and (f) top view. Scale bar: 10 mm.

Both HPMCAS and PEG 6000 showed thermal stability till ~ 200^{o}C. RFC/HPMCAS/PEG mixtures with 25% and 35% drug load did not exhibit significant weight loss below ~ 200^{o}C. Therefore, the process temperature needed to be maintained below 170^{o}C for INZ/HPC formulations and 200^{o}C for the two RFC/HPMCAS/PEG formulations to avoid degradation. Furthermore, feeding rate and screw speed of the extrusion process were optimized to generate filaments with a consistent thickness at 2.6 – 2.9 mm, which was found to facilitate 3D printing. The selected extrusion process parameters are presented in Table 1 in supplementary material. The resulting filaments were analysed to assure impurity levels remained minimum following extrusion. The INZ/HPC and RFC/HPMCAS/PEG filaments were sequentially 3D printed into tablets at 130^{o}C and 170^{o}C, respectively.

According to the theoretical drug loading the anticipated amounts for IZN and RFC in the extruded filaments were 25 and 35% respectively. However, the HPLC analysis showed less

drug content of 24% (IZN) and 29.75 (RFC). The reduction of drug amounts in the extruded filaments has been also reported by Genina and it was attributed to the stickiness of the drugs in the extruder barrels. However, the drug losses depend on the actual extruded batch amounts and the length of the extruder.

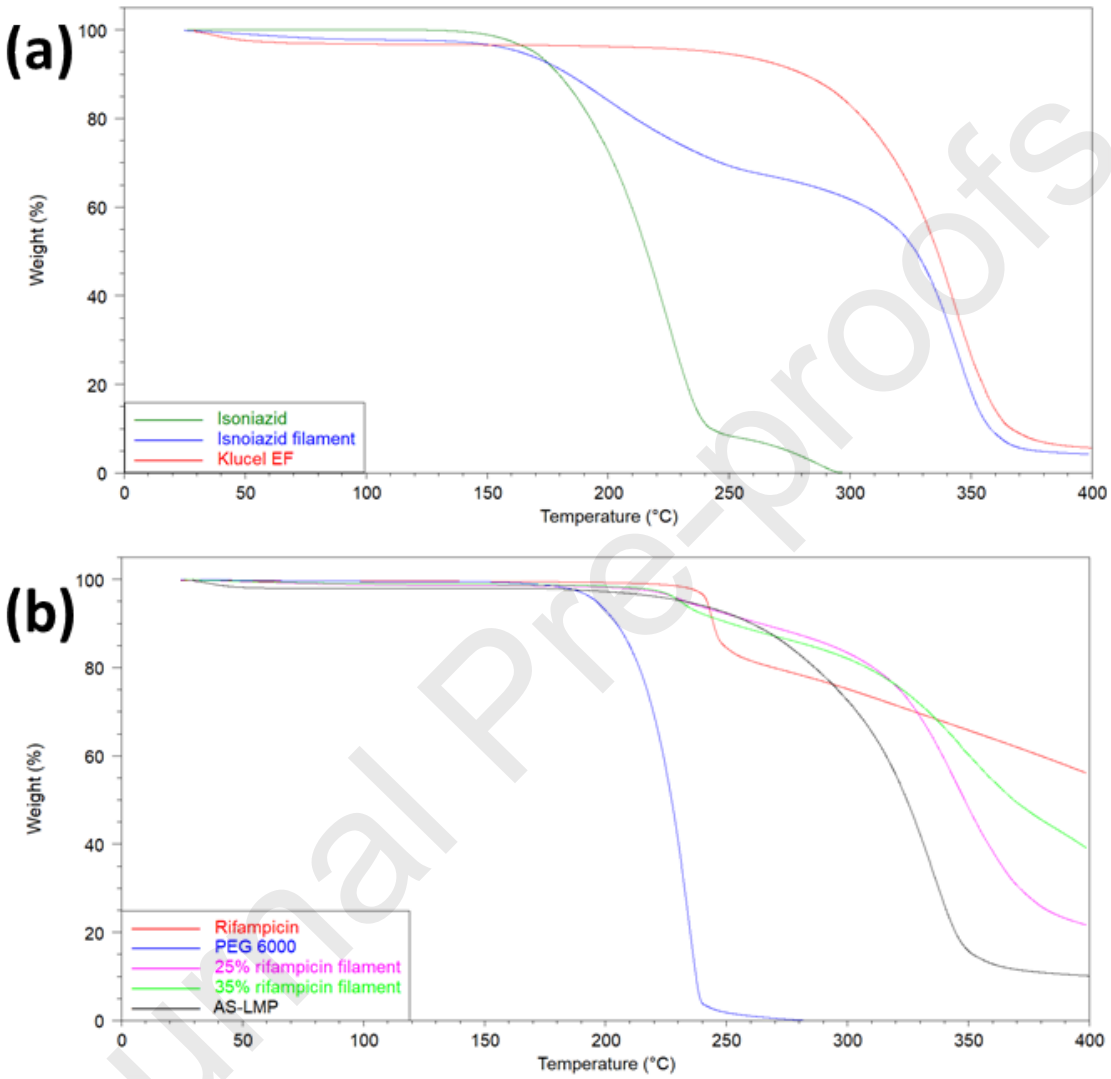

Fig. 3:*TGA thermograms of (a) Isoniazid, HPC EF, Isoniazid 3D printing filament, (b) HPMCAS AS-LMP, PEG 6000, Rifampicin, 25% and 35% rifampicin loaded filament.*

3.2 Solid state characterization of the filaments

X-Ray powder diffraction patterns of RFC/HPMCAS/PEG filament and each of its individual components were collected to identify the physical state of drug substance in the extruded filaments (Fig. 4a, b). The XRPD pattern of HPMCAS only exhibited broad humps due to its amorphous state. PEG 6000 had two characteristic diffraction peaks at 19º and 24º/2 θ . RFC drug substance had sharp diffraction peaks at 7.2°, 8.7°, 11.9°, 13.7°, 14.5°, 16.2°, 18.3° and

21.2°/2θ, which suggested the crystalline RFC was received as polymorph I, its thermodynamically most stable form.

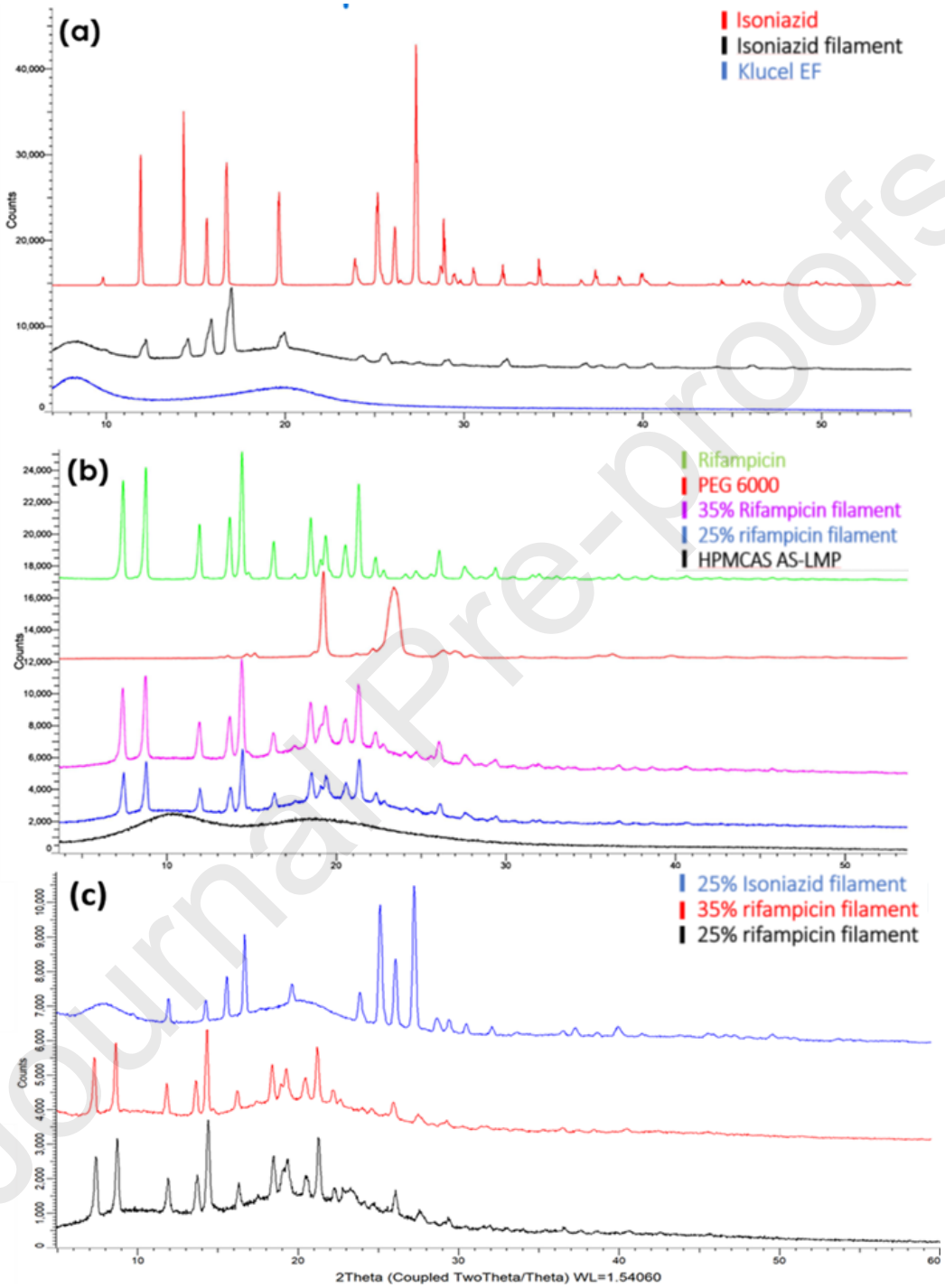

Fig. 4: *XRD graphs of (a) Isoniazid, Klucel EF, Isoniazid 3D printing filament, (b) rifampicin, PEG6000, HMPCAS AS-LMP, 25% drug loaded rifampicin 3D printing filament and 35% drug loaded rifampicin 3D printing filament. (c) XRD graphs of the filaments after 6 months.*

Journal Pre-proofs

The XRPD patterns of the RFC/HPMCAS/PEG filaments were found to have all characteristic diffraction peaks of crystalline polymorph I of RFC. The diffraction peaks of RFC in the filament only slightly broadened comparing to that of the drug alone suggested that majority of RFC remained as the same crystalline solid form in the extruded filament (Figure 4a). On the contrary, PEG 6000 most likely converted into its amorphous phase during extrusion because the characteristic diffraction peaks of PEG 6000 was not observed in the XRPD pattern of the extruded filament.

The DSC curves of the RFC/HPMCAS/PEG and its individual component are compared in Figure 5. PEG 6000 showed a melting endotherm at 59.78^{o}C. RFC exhibited a melting endotherm immediately followed by a decomposition exotherm at ~ 245^{o}C, which agreed with the thermal behaviour of the polymorph I of RFC reported previously. HPMCAS, as a non-crystalline polymer, has a glass transition temperature (Tg) at ~ 119.78^{o}C (Fig. 5b). While the extruded RFC/HPMCAS/PEG filaments were heated, melting endotherm of PEG 6000 was not observed. This observation confirmed that PEG 6000 was in its amorphous phase in the filament. Further heated, both filaments exhibited a glass transition at ~ 107^{o}C, which can be attributed to the glass transition of HPMCAS. As shown in Fig 5c, the lower glass transition temperatures (Tg) of the polymer in the filaments comparing to that of the polymer alone is unlikely due to the miscibility of PEG 6000 and HPMCAS. Otherwise, the low glass transition temperature of PEG 6000 (-22.71^{o}C) would significantly lower the resulting mixture (D'souza and Shegokar, 2016). The DSC curve of a placebo HPMCAS/PEG filament exhibited a glass transition temperature of ~116^{o}C, (Fig.2 in supplementary material) which confirmed the hypothesis. Small amount of RFC might have dissolved in the polymer, which shifted the glass transition temperatures of the RFC containing filaments lower. The two filaments with different drug loads exhibited the same glass transition temperatures suggested that HPMCAS polymer was saturated with RFC at both drug loads.

All characteristic diffraction peaks of crystalline INZ were found in the INZ/HPC filament (Fig. 4) at 12.1°, 14.3°, 15.5°, 16.5°, 19.7°, 24.2°, 25.6 ° and 27°/2θ. The diffraction peaks were found significantly weakened and broadened in the XRD patterns of the freshly prepared INZ/HPC filament. As shown in Fig 5a, the freshly prepared INZ/HPC filament exhibited a broad endotherm that started at ~145^{o}C and completed before the melting temperature of crystalline INZ, i.e. ~ 170.48^{o}C (Figure 5a).

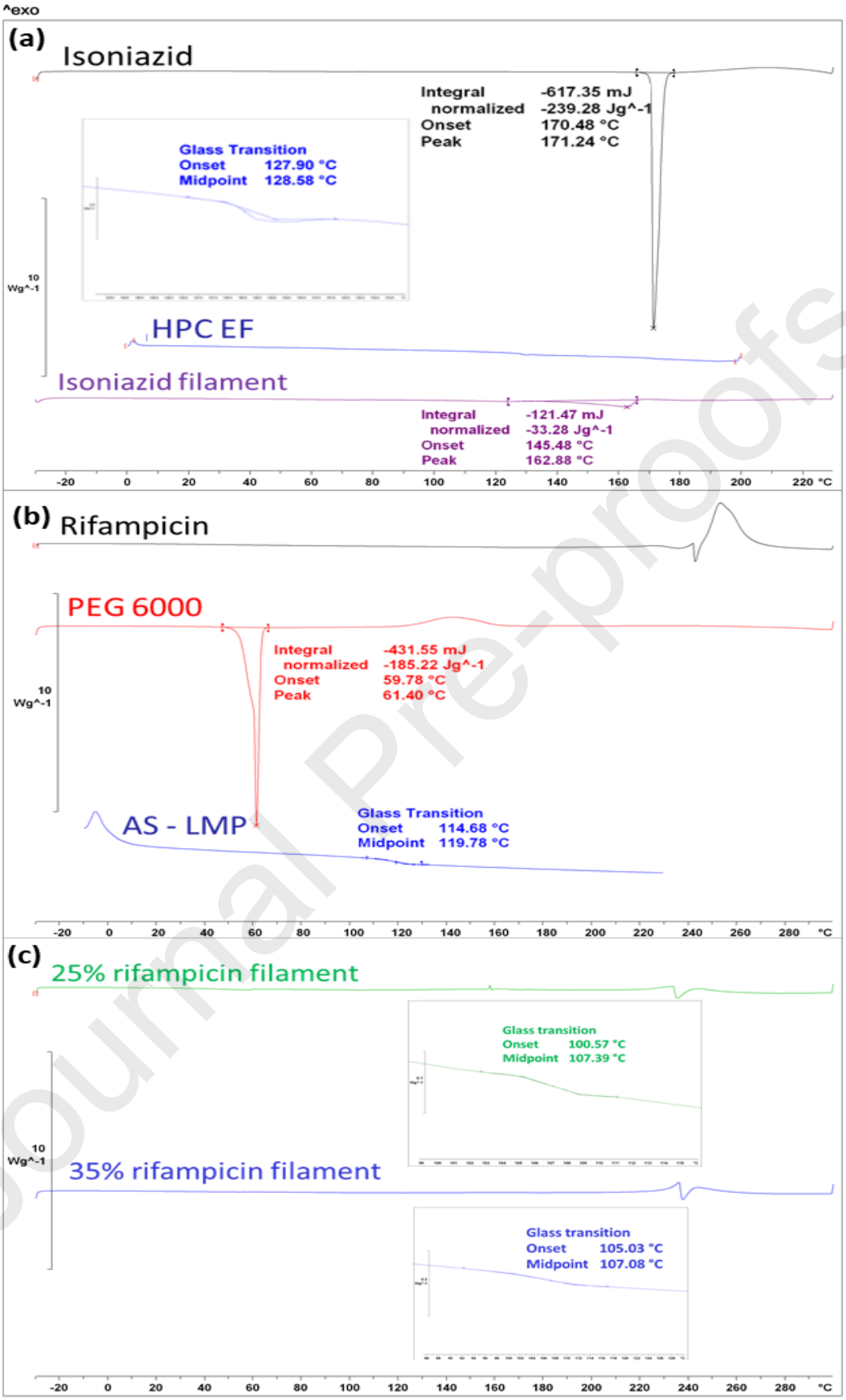

Fig. 5: *DSC thermograms of (a) Isoniazid, HPC-EF, Isoniazid loaded filament, (b) rifampicin, PEG 600, HPMCAS AS-LMP, (c) 25% rifampicin loaded and 35% rifampicin loaded filament .*

No melting endotherm of crystalline INZ was observed while the filament was heated. These observations suggested that appreciable amount of crystalline INZ dissolved in HPC during extrusion while crystalline INZ also existed in the freshly prepared filament. The diffraction peaks of crystalline INZ in the filament was sharpened over 6 months, which could attribute to crystallization of the dissolved INZ and the surface defects created during extrusion (Figure 4c).

3.3 Scanning electron microscopy

The extrusion process was optimized to generate filaments with a thickness of 2.6 – 2.9 mm, which ensured a consistent layer-by-layer deposition of formulation at a layer thickness of ~ 100 μm while 3D printed tablet.

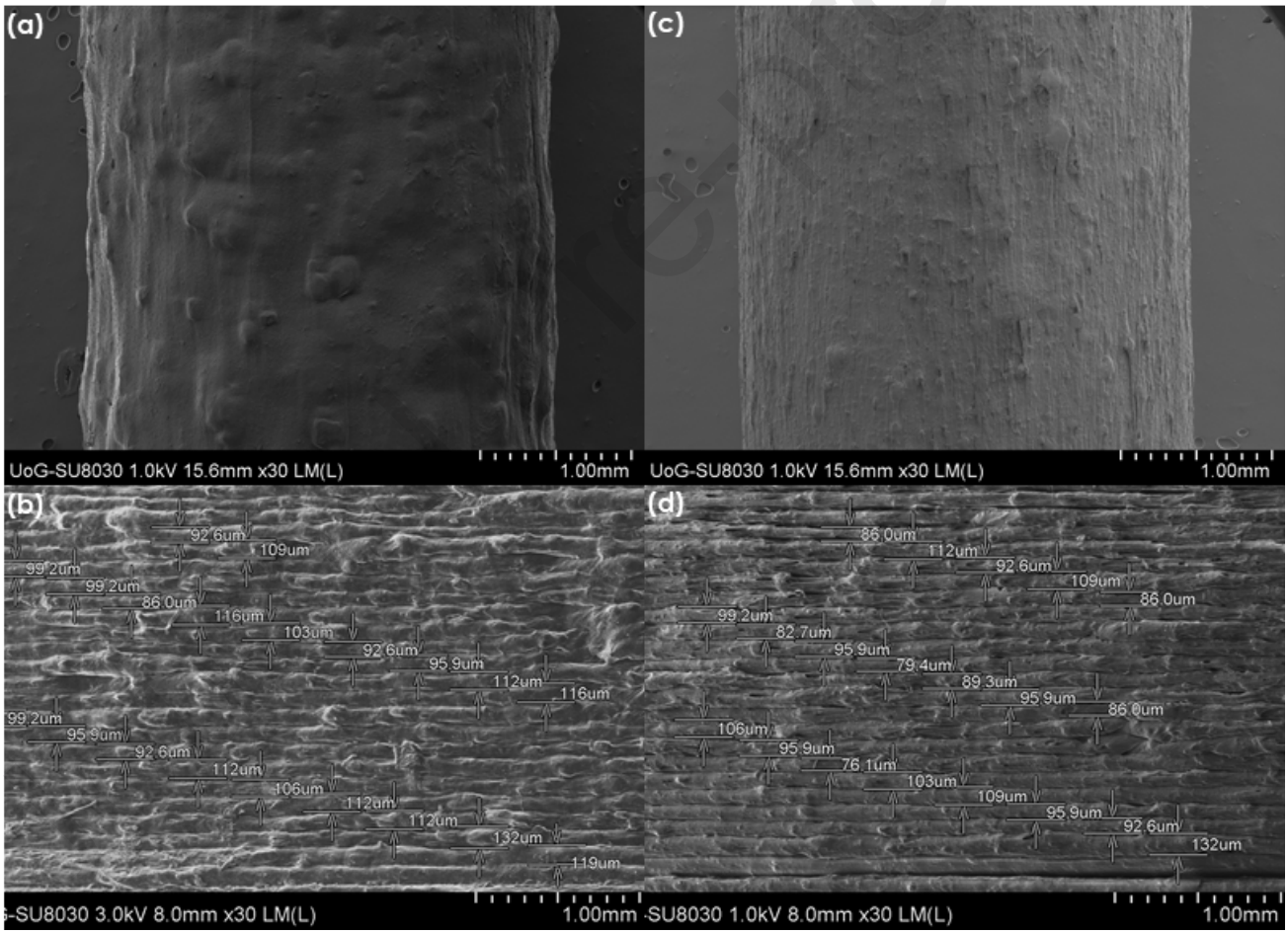

Fig. 6: *SEM images of (a)Isoniazid filament, (b) individual layer measurement of isoniazid caplet, (c) rifampicin filament and (d)individual layer measurement of rifampicin caplet.*

The thickness consistency of the extruded filaments was crucial to ensure high-quality prints of the caplets by avoiding under or over extrusion during the printing process. As shown in

Fig. 6, SEM images of the extruded filaments demonstrated reasonably smooth surface for INZ and RFC containing filaments. The SEM images of the 3D printed INZ/HPC and RFC/PEG/HPMCAS tablets also revealed the layered structure of the tablets with a consistent layer thickness of 96.2 ± 13.11 and 105.11 ± 11.41 μm, respectively

SEM/EDX is a known technique that determines elemental composition in micron–sized surfaces at 0.1% detection limit. The technique was used to analyse the distribution of INZ, RFC, and polymers within the extruded filaments (Fig. 7). All components in the formulations contain carbon (C) and oxygen (O) elements, while only INZ and RFC contain nitrogen (N) element. Therefore, comparing the images of C and O elements with that of N element reveals the distribution of the drugs in the polymer matrices.

Figure 7 has the SEM image of the cross-section of the INZ-containing filament (7a) and the distribution of C, O, and N elements across the filament (7(a), 7(b), and 7(c)). The SEM image of the filament revealed some spots in the surface in micron sizes. These spots were found to contain lower concentration of C and O elements (represented by the black spots in the images) but higher concentration of N element (represented by the darker red in the image). The comparison of the densities of C, O and N elements suggested that these spots are drug-rich regions in the filament. The presence of these drug-rich spots may be due to the recrystallization of INZ following extrusion. Recrystallization of INZ from its polymeric matrix most likely created elevated structure on the filament surface.

The SEM image of the cross-section of RFC containing filament, and the distribution of C, O, and N elements across the filament are also presented in Figure 7. The SEM image of the RFC-containing filament had smoother surface with fewer irregular spots comparing to the INZ-containing filament. These irregular spots had smaller sizes comparing to those found in the surface of the INZ-containing filament. Lower concentration of all three elements, i.e. C, O, and N, was found at these spots, which suggested these spots may be surface defects created during extrusion. Since majority of RFC remained as crystalline solid during extrusion, no recrystallization of RFC is expected on the surface.

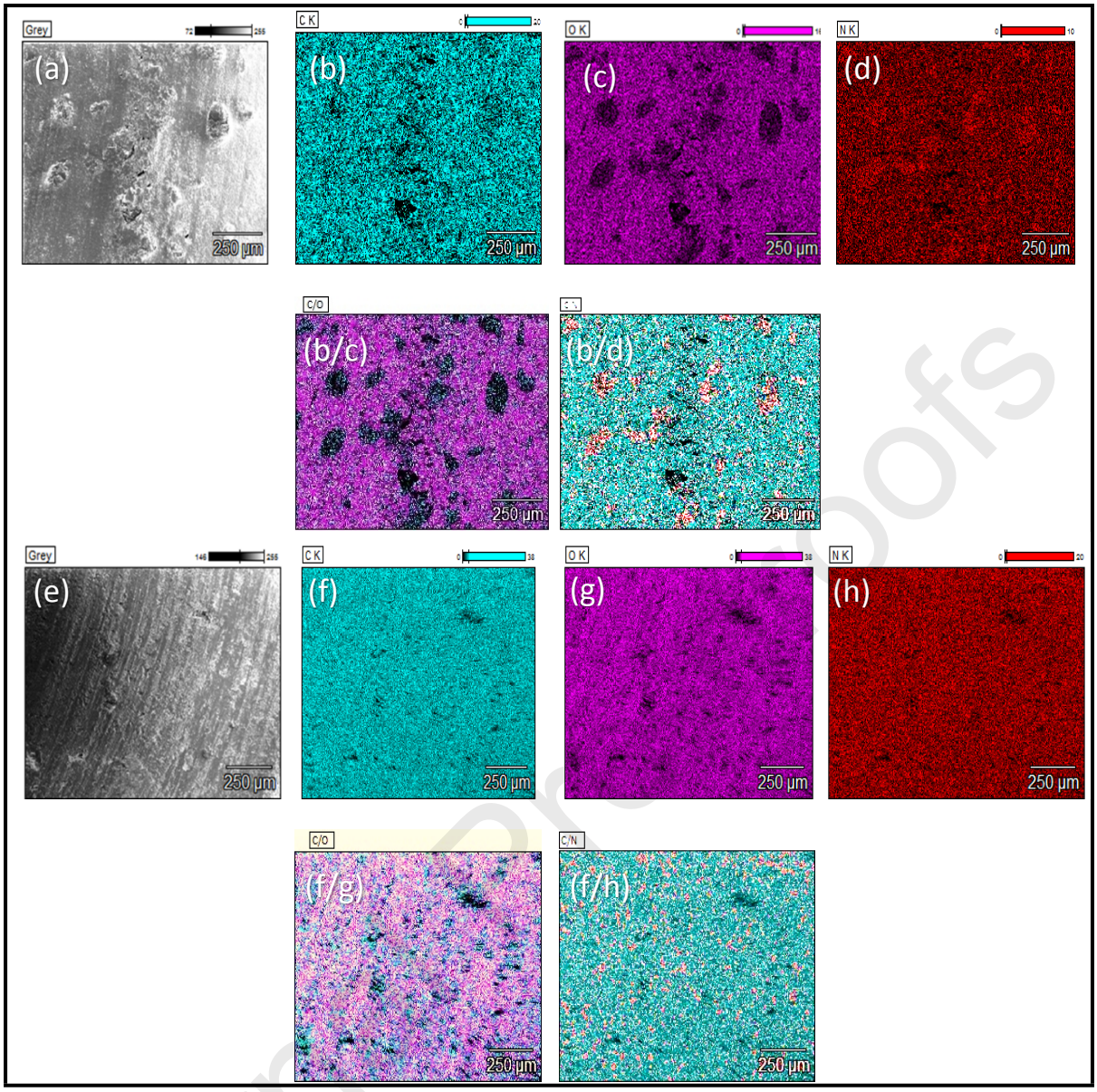

***Fig. 7**: Elemental mapping of extruded INZ/HPC (a,b,c,d) and RFC/HMPMC – AS filaments (e.f,g,h)*

3.4 Impact of tablet design on drug release

Drug release from the 3D printed tablets may be controlled by modifying the infill density of the tablets. The tablets with higher infill density, i.e. more empty spaces, have lower surface area, from which drug dissolves more slowly. Covering layers on the outer tablet surface can also affect the dissolution rates and result in delayed drug release.

INZ is a highly water-soluble drug, which dissolved completely in acidic medium (pH = 1.2) within 30 mins. The dissolution rate of INZ from the 3D printed INZ/HPC tablets was modified by adjusting infill density and number of covering layers (Fig. 8).

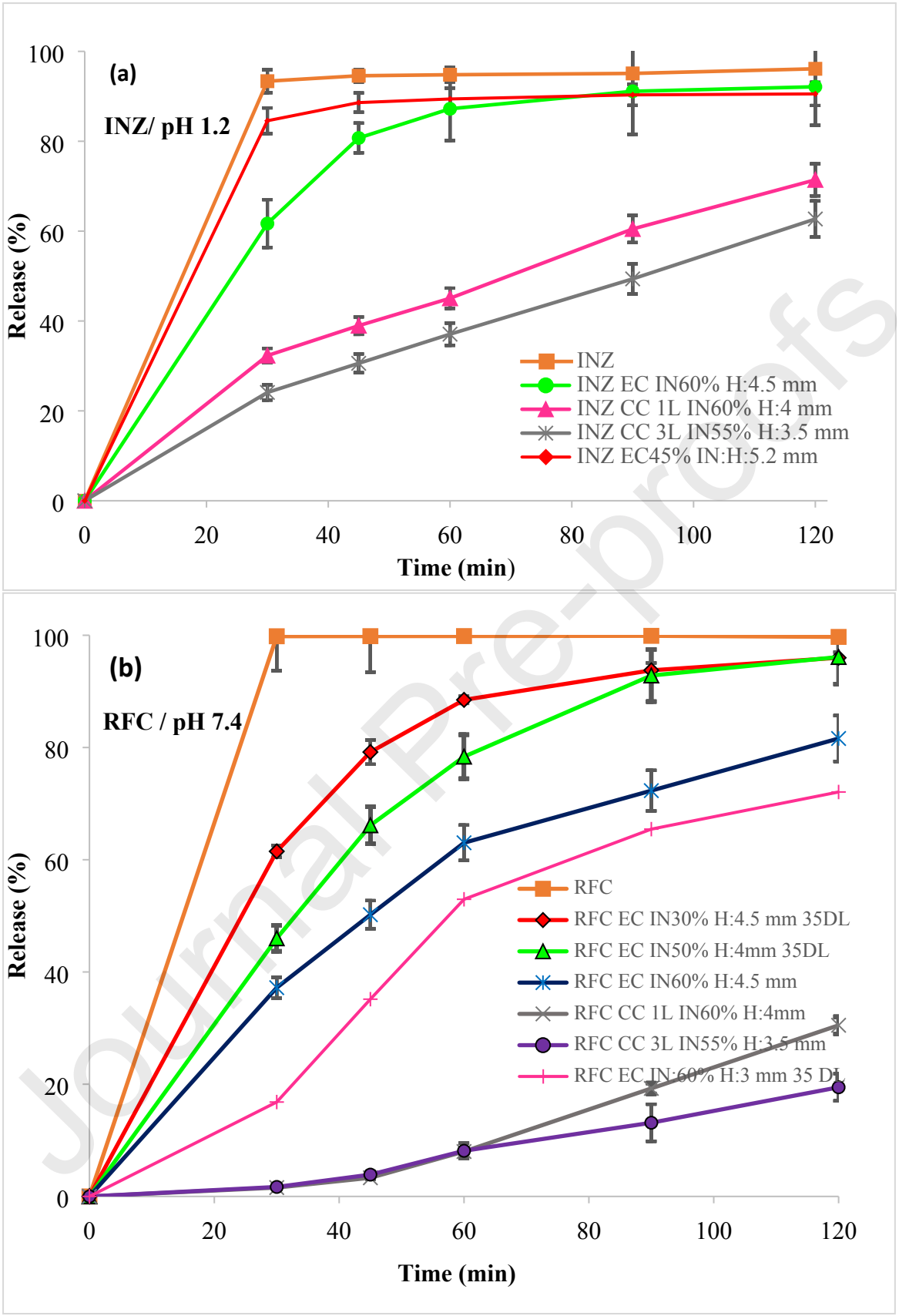

Fig. 8: *(a) release profile of INZ caplet in acidic pH and (b) release profile of RFC caplet in alkaline pH. EC: exposed caplet, CC: covered caplet, H: height, L: covering layers, IN: infill density and 35DL: 35% drug loading*

The tablet of Design 2 had one extra covering layer comparing to the tablet of Design 3. The former had a significantly slower dissolution, i.e. 32% release, comparing to the latter, which had 80% release in 45 mins. The impact of infill density on drug release was clearly illustrated by comparing the dissolution of the INZ/HPC tablets of Design 3 and Design 4. The dissolution of the tablets was decreased from 85% to 67% by increasing the infill density from 45% to 60% in 30 mins. Increasing number of covering layers as in the tablet of Design 1 further reduces drug release even the infill density was lower than that of Design 2. These observations demonstrated that both infill density and covering layers can be used to modify drug release from a 3D printed tablet, while covering layer may be a more effective way to reduce drug release.

RFC alone dissolved completely in pH 7.4 buffer within 30 mins. Similarly, the dissolution rate of RFC from the 3D printed RFC/HPMCAS/PEG tablets was modified by adjusting drug load, infill density, and number of covering layers (Figure 8). The tablet of Design 9 had ~ 79% release at 45 mins. The percentage drug release was reduced to ~ 66% (Design 8) and ~ 35% (Design 10) by increasing the infill density to 50% and 60%, respectively. The dissolution rate of the tablet of Design 6, applied with one covering layer, was found to be significantly lowered comparing to that of the tablet of Design 7, though all the other factors remained the same. Increasing number of covering layers as in the tablet of Design 5 further reduced drug release even the infill density was lower than that of Design 6. These observations again demonstrated that drug release from a 3D printed tablet can be reduced by increasing infill density and/or applying covering layers. The impact of RFC drug load on drug release can be illustrated by comparing the dissolution profiles of tablet with Design 7 and Design 10. Tablet of Design 10 with higher drug load had a slower dissolution than that of Design 7 with 25% drug load.

With the understanding of the impact of infill density, covering layer, and drug load, a bilayer tablet was designed and 3D-printed consisting INZ/HPC in one layer and RFC/PEG/HPMCAS in another. No covering layer (open designs) was applied to either layer to allow INZ and RFC to release quickly in acidic condition and basic condition, respectively. The INZ/HPC layer had a drug load of 25% and infill density of 45%. The RFC/PEG/HPMCAS layer had a drug load of 35% and infill density of 30%. The bilayer tablet had ~ 87% of INZ released in 45 mins at pH 1.2, which met the USP specification [28]. The release of RFC was delayed in the acidic media with less than 10% released in 120 mins. However, approximately ~ 76% of RFC was released in 45 mins after the dissolution media was changed to pH 7.4, which was comparable

to the dissolution rate at pH 1.0 stated in USP [29]. It is evident that a fixed dose combination drug product containing INZ and RFC may be 3D printed with careful design.

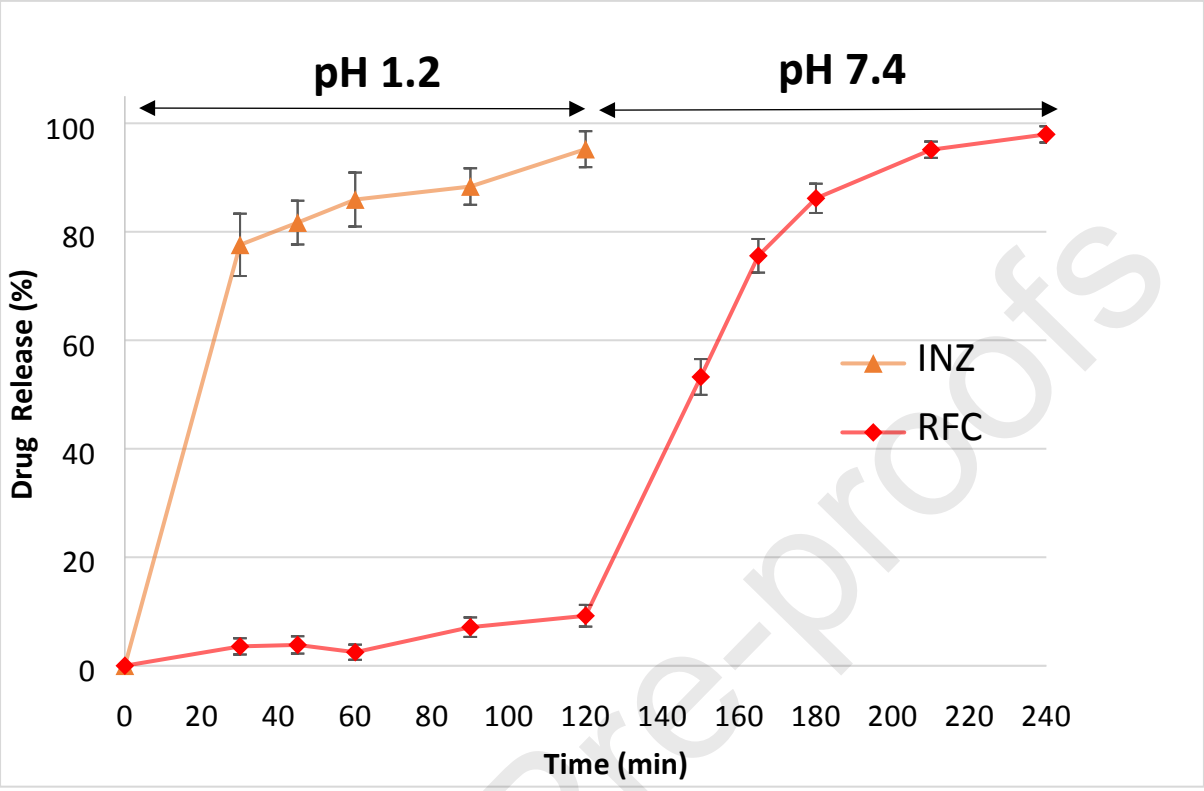

Fig. 9: *release profile of INZ/RFC tablets (open designs) in 0.1 N HCl (pH 1.2) for 120 min followed by release in pH 7.4.*

Conclusion

In this study FDM 3D printing technology was successfully employed to generate a bilayer tablet with two model drugs INZ and RFC for treatment of tuberculosis. The polymer type, drug load, infill density, and covering layers were carefully designed to achieve a fast release of INZ in acidic condition and a delayed release of RFC in alkaline conditions.

The impact of the design of the 3D printed tablets showed that the infill density and the number of covering layers played a key role on the release rates of drugs.

Overall, we showed that 3D printing can be employed to fabricate personalised bilayer tablets with release of each API at different pH values to avoid degradation due to drug – drug interactions. Furthermore, depending on patients' needs the drug dose can be adjusted either by the tablet design or the API loading of the filament and potentially lead to efficient treatment of tuberculosis.

Journal Pre-proofs

References

Aho, J., Bøtker, J.P., Genina, N., Edinger, M., Arnfast, L., Rantanen, J., 2019. Roadmap to 3D-Printed Oral Pharmaceutical Dosage Forms: Feedstock Filament Properties and Characterization for Fused Deposition Modeling. J. Pharm. Sci. 108, 26–35. https://doi.org/https://doi.org/10.1016/j.xphs.2018.11.012

Bangalore, S., Kamalakkannan, G., Parkar, S., Messerli, F.H., 2007. Fixed-Dose Combinations Improve Medication Compliance: A Meta-Analysis. Am. J. Med. 120, 713–719. https://doi.org/https://doi.org/10.1016/j.amjmed.2006.08.033

Blomberg, B., Spinaci, S., Fourie, B., Laing, R., 2001. The rationale for recommending fixed-dose combination tablets for treatment of tuberculosis. Bull. World Health Organ. 79, 61–68.

Boetker, J., Water, J.J., Aho, J., Arnfast, L., Bohr, A., Rantanen, J., 2016. Modifying release characteristics from 3D printed drug-eluting products. Eur. J. Pharm. Sci. 90, 47–52. https://doi.org/https://doi.org/10.1016/j.ejps.2016.03.013

Castellano, J.M., Sanz, G., Peñalvo, J.L., Bansilal, S., Fernández-Ortiz, A., Alvarez, L., Guzmán, L., Linares, J.C., García, F., D'Aniello, F., Arnáiz, J.A., Varea, S., Martínez, F., Lorenzatti, A., Imaz, I., Sánchez-Gómez, L.M., Roncaglioni, M.C., Baviera, M., Smith, S.C., Taubert, K., Pocock, S., Brotons, C., Farkouh, M.E., Fuster, V., 2014. A Polypill Strategy to Improve Adherence: Results From the FOCUS Project. J. Am. Coll. Cardiol. 64, 2071–2082. https://doi.org/https://doi.org/10.1016/j.jacc.2014.08.021

Chai, X., Chai, H., Wang, X., Yang, J., Li, J., Zhao, Y., Cai, W., Tao, T., Xiang, X., 2017. Fused Deposition Modeling (FDM) 3D Printed Tablets for Intragastric Floating Delivery of Domperidone. Sci. Rep. 7, 2829. https://doi.org/10.1038/s41598-017-03097-x

D'souza, A.A., Shegokar, R., 2016. Polyethylene glycol (PEG): a versatile polymer for pharmaceutical applications. Expert Opin. Drug Deliv. 13, 1257–1275. https://doi.org/10.1080/17425247.2016.1182485

Deardorff, W.J., Grossberg, G.T., 2016. A fixed-dose combination of memantine extended-release and donepezil in the treatment of moderate-to-severe Alzheimer's disease. Drug Des. Devel. Ther. 10, 3267–3279. https://doi.org/10.2147/DDDT.S86463

El Aita, I., Breitkreutz, J., Quodbach, J., 2019. On-demand manufacturing of immediate release levetiracetam tablets using pressure-assisted microsyringe printing. Eur. J. Pharm. Biopharm. 134, 29–36. https://doi.org/https://doi.org/10.1016/j.ejpb.2018.11.008

Fina, F., Goyanes, A., Gaisford, S., Basit, A.W., 2017. Selective laser sintering (SLS) 3D printing of

medicines. Int. J. Pharm. 529, 285–293. https://doi.org/https://doi.org/10.1016/j.ijpharm.2017.06.082

Fina, F., Goyanes, A., Madla, C.M., Awad, A., Trenfield, S.J., Kuek, J.M., Patel, P., Gaisford, S., Basit, A.W., 2018. 3D printing of drug-loaded gyroid lattices using selective laser sintering. Int. J. Pharm. 547, 44–52. https://doi.org/https://doi.org/10.1016/j.ijpharm.2018.05.044

Genina, N., Boetker, J.P., Colombo, S., Harmankaya, N., Rantanen, J., Bohr, A., 2017. Anti-tuberculosis drug combination for controlled oral delivery using 3D printed compartmental dosage forms: From drug product design to in vivo testing. J. Control. Release 268, 40–48. https://doi.org/https://doi.org/10.1016/j.jconrel.2017.10.003

Gioumouxouzis, C.I., Baklavaridis, A., Katsamenis, O.L., Markopoulou, C.K., Bouropoulos, N., Tzetzis, D., Fatouros, D.G., 2018. A 3D printed bilayer oral solid dosage form combining metformin for prolonged and glimepiride for immediate drug delivery. Eur. J. Pharm. Sci. 120, 40–52. https://doi.org/https://doi.org/10.1016/j.ejps.2018.04.020

Gioumouxouzis, C.I., Tzimtzimis, E., Katsamenis, O.L., Dourou, A., Markopoulou, C., Bouropoulos, N., Tzetzis, D., Fatouros, D.G., 2020. Fabrication of an osmotic 3D printed solid dosage form for controlled release of active pharmaceutical ingredients. Eur. J. Pharm. Sci. 143, 105176. https://doi.org/https://doi.org/10.1016/j.ejps.2019.105176

Gohel, M.C., Sarvaiya, K.G., 2007. A novel solid dosage form of rifampicin and isoniazid with improved functionality. AAPS PharmSciTech 8, E133–E139. https://doi.org/10.1208/pt0803068

Goyanes, A., Buanz, A.B.M., Hatton, G.B., Gaisford, S., Basit, A.W., 2015a. 3D printing of modified-release aminosalicylate (4-ASA and 5-ASA) tablets. Eur. J. Pharm. Biopharm. 89, 157–162. https://doi.org/https://doi.org/10.1016/j.ejpb.2014.12.003

Goyanes, A., Wang, J., Buanz, A., Martínez-Pacheco, R., Telford, R., Gaisford, S., Basit, A.W., 2015b. 3D Printing of Medicines: Engineering Novel Oral Devices with Unique Design and Drug Release Characteristics. Mol. Pharm. 12, 4077–4084. https://doi.org/10.1021/acs.molpharmaceut.5b00510

Horsburgh, C.R., Barry, C.E., Lange, C., 2015. Treatment of Tuberculosis. N. Engl. J. Med. 373, 2149–2160. https://doi.org/10.1056/NEJMra1413919

Jamróz, W., Kurek, M., Czech, A., Szafraniec, J., Gawlak, K., Jachowicz, R., 2018. 3D printing of tablets containing amorphous aripiprazole by filaments co-extrusion. Eur. J. Pharm. Biopharm. 131, 44–47. https://doi.org/https://doi.org/10.1016/j.ejpb.2018.07.017

Kyobula, M., Adedeji, A., Alexander, M.R., Saleh, E., Wildman, R., Ashcroft, I., Gellert, P.R.,

Roberts, C.J., 2017. 3D inkjet printing of tablets exploiting bespoke complex geometries for controlled and tuneable drug release. J. Control. Release 261, 207–215. https://doi.org/https://doi.org/10.1016/j.jconrel.2017.06.025

Melocchi, A., Uboldi, M., Inverardi, N., Briatico-Vangosa, F., Baldi, F., Pandini, S., Scalet, G., Auricchio, F., Cerea, M., Foppoli, A., Maroni, A., Zema, L., Gazzaniga, A., 2019. Expandable drug delivery system for gastric retention based on shape memory polymers: Development via 4D printing and extrusion. Int. J. Pharm. 571, 118700. https://doi.org/10.1016/j.ijpharm.2019.118700

Michael, S., Sorg, H., Peck, C.-T., Koch, L., Deiwick, A., Chichkov, B., Vogt, P.M., Reimers, K., 2013. Tissue Engineered Skin Substitutes Created by Laser-Assisted Bioprinting Form Skin-Like Structures in the Dorsal Skin Fold Chamber in Mice. PLoS One 8, e57741.

Nasereddin, J.M., Wellner, N., Alhijjaj, M., Belton, P., Qi, S., 2018. Development of a Simple Mechanical Screening Method for Predicting the Feedability of a Pharmaceutical FDM 3D Printing Filament. Pharm. Res. 35, 151. https://doi.org/10.1007/s11095-018-2432-3

Öblom, H., Zhang, J., Pimparade, M., Speer, I., Preis, M., Repka, M., Sandler, N., 2019. 3D-Printed Isoniazid Tablets for the Treatment and Prevention of Tuberculosis—Personalized Dosing and Drug Release. AAPS PharmSciTech 20, 52. https://doi.org/10.1208/s12249-018-1233-7

Pereira, B.C., Isreb, A., Forbes, R.T., Dores, F., Habashy, R., Petit, J.-B., Alhnan, M.A., Oga, E.F., 2019. 'Temporary Plasticiser': A novel solution to fabricate 3D printed patient-centred cardiovascular 'Polypill' architectures. Eur. J. Pharm. Biopharm. 135, 94–103. https://doi.org/https://doi.org/10.1016/j.ejpb.2018.12.009

Pietrzak, K., Isreb, A., Alhnan, M.A., 2015. A flexible-dose dispenser for immediate and extended release 3D printed tablets. Eur. J. Pharm. Biopharm. 96, 380–387. https://doi.org/https://doi.org/10.1016/j.ejpb.2015.07.027

Sadia, M., Arafat, B., Ahmed, W., Forbes, R.T., Alhnan, M.A., 2018. Channelled tablets: An innovative approach to accelerating drug release from 3D printed tablets. J. Control. Release 269, 355–363. https://doi.org/https://doi.org/10.1016/j.jconrel.2017.11.022

Sadia, M., Sośnicka, A., Arafat, B., Isreb, A., Ahmed, W., Kelarakis, A., Alhnan, M.A., 2016. Adaptation of pharmaceutical excipients to FDM 3D printing for the fabrication of patient-tailored immediate release tablets. Int. J. Pharm. 513, 659–668. https://doi.org/https://doi.org/10.1016/j.ijpharm.2016.09.050

Scoutaris, N., Ross, S.A., Douroumis, D., 2018. 3D Printed "Starmix" Drug Loaded Dosage Forms for Paediatric Applications. Pharm. Res. 35, 34. https://doi.org/10.1007/s11095-017-2284-2

Shishoo, C.J., Shah, S.A., Rathod, I.S., Savale, S.S., Vora, M.J., 2001a. Impaired bioavailability of rifampicin in presence of isoniazid from fixed dose combination (FDC) formulation. Int. J. Pharm. 228, 53–67. https://doi.org/https://doi.org/10.1016/S0378-5173(01)00831-6

Shishoo, C.J., Shah, S.A., Rathod, I.S., Savale, S.S., Vora, M.J., 2001b. Impaired bioavailability of rifampicin in presence of isoniazid from fixed dose combination (FDC) formulation. Int. J. Pharm. 228, 53–67. https://doi.org/https://doi.org/10.1016/S0378-5173(01)00831-6

Siamidi, A., Tsintavi, E., Rekkas, D., Vlachou, M., 2020. 3D-Printed Modified-Release Tablets: A Review of the Recent Advances.

Trenfield, S.J., Awad, A., Goyanes, A., Gaisford, S., Basit, A.W., 2018. 3D Printing Pharmaceuticals: Drug Development to Frontline Care. Trends Pharmacol. Sci. 39, 440–451. https://doi.org/https://doi.org/10.1016/j.tips.2018.02.006

Zema, L., Melocchi, A., Maroni, A., Gazzaniga, A., 2017. Three-Dimensional Printing of Medicinal Products and the Challenge of Personalized Therapy. J. Pharm. Sci. 106, 1697–1705. https://doi.org/10.1016/j.xphs.2017.03.021

Journal Pre-proofs

Supplementary material

Table 1- Hot melt extrusion processing parameters for fabrication of drug loaded 3D printing filaments

Formulation	Ratio	Zone 1 (°C)	Zone 2 (°C)	Zone 3 (°C)	Zone 4 (°C)	Zone 5 (°C)	Zone 6 (°C)	Zone 7 (°C)	Zone 8 (°C)	Zone 9 (°C)	Die (°C)	Screw speed (rpm)
INZ/Klucel EF	25:75	80	100	130	150	160	160	150	160	160	150	50
RFC/AS-LMP/PEG6000	25:55:20	40	55	100	150	150	150	150	150	150	120	50
RFC/AS-LMP/PEG6000	35:45:20	40	55	100	150	150	150	150	150	150	120	50

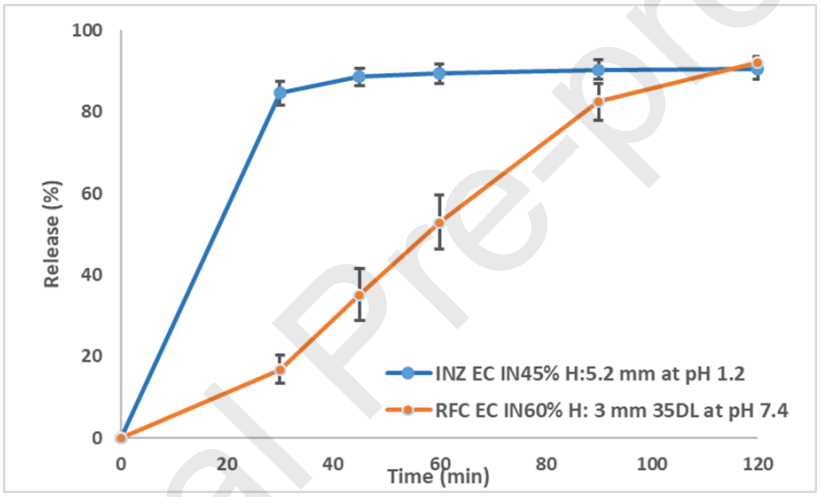

Fig1. release profiles of 3D printed design 4 at pH 1.2 and design 8 at pH 7.4

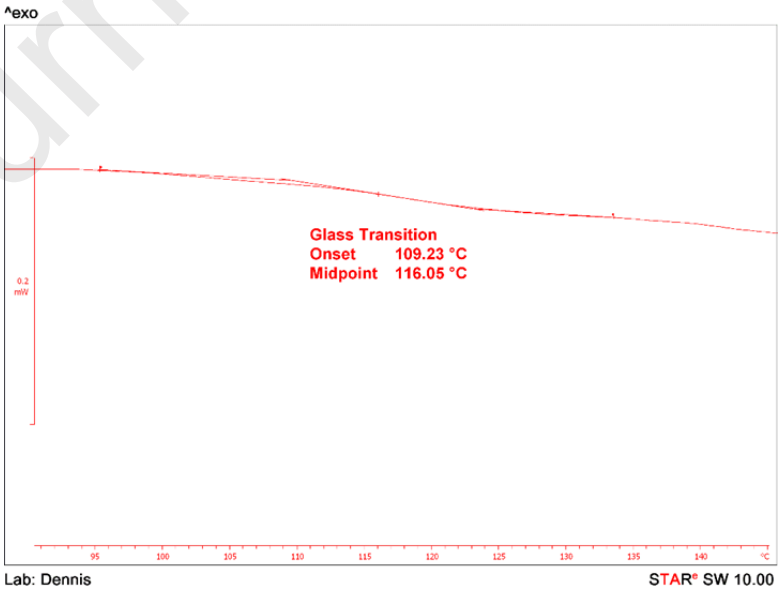

Fig2.- DSC thermogram of HPMCAS/PEG placebo filament

Journal Pre-proofs

Graphical abstract

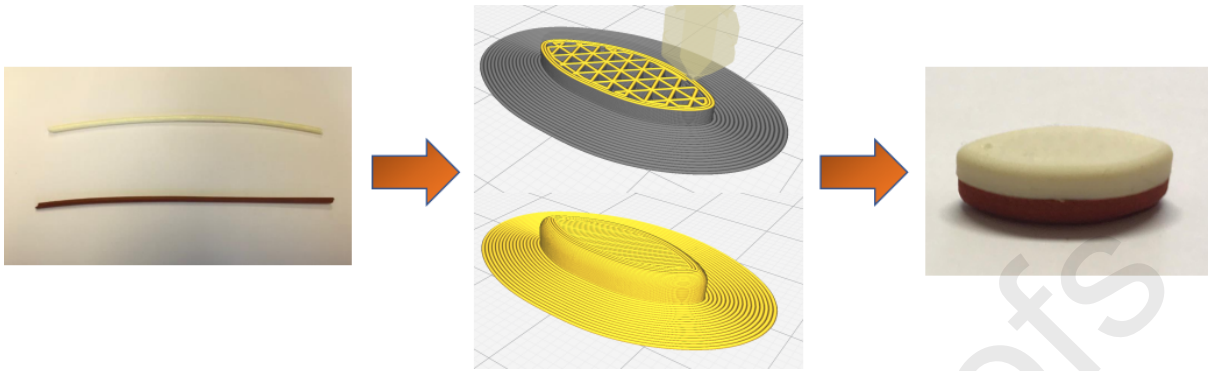

Journal Pre-proofs

Credit authors statement

Conceptualization: Douroumis,

Methodology: Ghanizadeh Douroumis, Kumar

Validation: Ghanizadeh, Hurt: Validation, formal anlysis, investigation

Formal analysis: Ghanizadeh, Hurt

Investigation: Ghanizadeh

Writing - Original Draft: Ghanizadeh, Gong, Douroumis

Visualization: Ghanizadeh, Gong, Karki, Hui

Supervision: Kumar, Gong, Karki, Hui, Douroumis

Project administration: Douroumis, Kumar, Gong, Hui

Funding acquisition: Bristol Myers Squibb (formerly Celgene Corporation)

Journal Pre-proofs